

1

# The perpetual fragility of creeping hillslopes

2

3 Nakul S. Deshpande<sup>1</sup>, David J. Furbish<sup>2,3</sup>, Paulo E. Arratia<sup>4</sup>, and Douglas J. Jerolmack<sup>1,4</sup>

4

5 <sup>1</sup>*Department of Earth and Environmental Science, University of Pennsylvania, Philadelphia, Pennsylvania, USA*

6

7 <sup>2</sup>*Departments of Earth and Environmental Sciences Vanderbilt University, Nashville, Tennessee, USA*

8

9 <sup>3</sup>*Civil and Environmental Engineering, Vanderbilt University, Nashville, Tennessee, USA*

10

11 <sup>4</sup>*Department of Mechanical Engineering & Applied Mechanics, University of Pennsylvania, Philadelphia, Pennsylvania, USA*

12

13 May 14, 2020

14

## 15 Abstract

16

17 Soil-mantled hillslopes owe their smooth, convex shape to creep<sup>1,2</sup>; the slow and persistent, gravity-driven motion of grains on slopes below the angle of repose. Existing models presume that soil creep occurs via mechanical displacement of grains by (bio)physical disturbances<sup>3,4</sup>. Recent simulations<sup>5</sup>, however, suggest that soil can creep without these disturbances, due to internal relaxation dynamics characteristic of disordered and fragile solids such as glass. Here we report experimental observations of creeping motion in an undisturbed sandpile, at micron resolution over timescales of  $10^0 - 10^6$  s, for a variety of natural and synthetic granular materials. We observe two behaviors typically associated with creeping glass: strain occurs as localized and spatially-heterogeneous grain motions<sup>6</sup>; and creep rates decay as a power-law function of time<sup>7</sup>. Further, creep can be accelerated or suppressed by thermal cycles and shaking, respectively. Averaged strain profiles decay exponentially with depth, in agreement with field observations of creeping hillslope soils<sup>8-10</sup>. Our findings demonstrate that soil is fragile in terms of sensitivity to disturbances, but that creep dynamics are robust across grains and glasses. Mapping soil creep to the more generic glass problem provides a new framework for modeling hillslope sediment transport, and new insights on the nature of yield and failure.

18

19

20

21

22

23

24

25

26

27

28 **Keywords**— geomorphology, granular physics, glassy dynamics, relaxation and rejuvenation, aging

29

30

## 28 Introduction

29 The shapes of hills encode a signature of tectonics, climate and life, through the influence of these processes on  
30 sediment transport<sup>4,11–13</sup>. Soil fails by landslides on the steepest slopes, leaving telltale scars on the landscape. Below  
31 the angle of repose, however, soil-mantled hillslopes are characteristically smooth and convex<sup>4,13</sup>. Although this soil  
32 is considered a solid, it appears to flow over geologic time in a process called soil creep<sup>14,15</sup>. What is the mechanism  
33 for granular motion below the angle of repose? This has been speculated on for over 100 years<sup>1,2</sup>. Modern treatments  
34 trace their origin to Culling<sup>3</sup>, who envisioned that the net effect of environmental disturbances (biological, hydrological  
35 and physical) acting on and within soil was to inject porosity, which facilitates particle motion. He also recognized  
36 that porosity, and the associated particle activity, must diminish with depth. In the continuum limit Culling proposed  
37 a diffusion-like relation between sediment flux and topographic gradient, that has been elaborated on by many authors  
38 and implemented in virtually all landscape evolution models<sup>4,13,15–18</sup>. Remarkably, the hypothesized grain motions  
39 in Culling’s model have never been experimentally examined. More broadly, Culling’s mathematical formulation  
40 corresponds to a physical picture of soil as a peculiar kind of “granular gas” (Supplementary Materials Section S1)  
41 that is inconsistent with known granular mechanics. Researchers have begun to recognize the need to understand  
42 grain-scale dynamics, in order to derive physically-informed models of soil mixing and transport on hillslopes<sup>19,20</sup>.  
43 While tracers have been used for over 60 years to measure coarse profiles of soil displacement on hillslopes<sup>14</sup>, the slow  
44 and erratic nature of creep has prevented direct observation of grain motions in the field. The canonical hillslope  
45 laboratory experiment of Roering and colleagues<sup>21</sup> showed how acoustic noise can induce grain motion below the  
46 angle of repose; however, our reanalysis indicates that grains were actually fluidized into inertial flows, rather than  
47 sub-critical creep (Fig. S1).

48 Creep has also been recognized in the context of dense granular flows. These flows have been modeled with a local  
49 ‘ $\mu(I)$  rheology’ where the effective friction ( $\mu$ ) is a function of a dimensionless shear rate called the inertial number,  
50  $I \equiv \dot{\epsilon}d/\sqrt{P/\rho}$ , where  $\dot{\epsilon}$  is shear rate,  $d$  is grain size,  $P$  is confining pressure and  $\rho$  is density<sup>22</sup>. Inertial flows transition  
51 at depth to a slow creep regime, characterized by intermittent and apparently random particle motions<sup>23,24</sup> and  
52 exponential velocity profiles<sup>25,26</sup>. Recent experiments and simulations suggest the transition to creep occurs below  
53  $I \sim 10^{-5}$  (refs.<sup>5,26,27</sup>). The local  $\mu(I)$  rheology predicts that grains should be static below yield, and therefore  
54 cannot describe the creep regime<sup>26</sup>. To account for creep, nonlocal models have been proposed in which fluidized  
55 motions from the inertial regime diffuse downward into the bulk<sup>28</sup>. However, recent experiments have revealed creep  
56 in the absence of a flowing layer<sup>29,30</sup>. Observations in a progressively tilted sandbox showed that, on approach to  
57 the angle of repose, sporadic and localized grain motions became more frequent and eventually linked up to affect  
58 yield<sup>29</sup>. Granular simulations have reproduced these behaviors without any imposed disturbances<sup>5</sup>. The addition of  
59 low-amplitude ( $\ll d$ ), random perturbations accelerated simulated creep rates, but did not qualitatively change the  
60 dynamics<sup>5,31</sup>; however, the spectrum of disturbances explored in these models is quite limited.

61 Creep in amorphous solids, such as glass, is associated with sub-yield plastic deformation in response to an  
62 applied stress<sup>6</sup>. A unifying characteristic of amorphous solids is that they are fragile: any particle configuration is  
63 metastable, and very small perturbations can lead to structural rearrangements<sup>27,32</sup>. These creep motions are manifest  
64 as spatially heterogeneous, mesoscopic (length  $\gg d$ ) zones of strain<sup>6</sup>. In glasses, relaxation by plastic rearrangements  
65 leads to aging; rigidity increases with time, leading to a slow down in creep rates. This decline in plasticity can  
66 be reversed by rejuvenation, typically by changing temperature<sup>33</sup>. There is emerging evidence that granular creep  
67 shares deep similarities with glasses<sup>5,27</sup>, and theorists have proposed that mechanical noise in granular systems may  
68 modulate creep in an analogous manner to thermal fluctuations in glasses<sup>7,34</sup>. No experiments, however, have been  
69 conducted to test these ideas. In this study we examine creep dynamics of an undisturbed sub-critical sandpile,  
70 probing grain motions through time using an optical technique that allows us to observe exceedingly slow strain  
71 rates. Creep behavior in the sandpile exhibits all of the hallmarks of relaxation in glassy materials. We also explore  
72 how disturbances can enhance or reverse aging, completing the picture of soil creep as relaxation and rejuvenation of a  
73 fragile solid and illustrating that in the natural environment, hillslopes are made perpetually fragile by environmental  
74 perturbations. Comparisons of experimental creep profiles with data from natural hillslopes indicate that laboratory  
75 observations are generalizable.

## Undisturbed creep results

Our first objective is to demonstrate the existence of creep in a minimally-disturbed model hillslope. Based on previous work<sup>5,23,25,26,29</sup>, we expect creep rates to be exceedingly slow ( $\leq 10^{-6} m/s$ ) which makes typical particle tracking methods impractical. Instead, we measure grain motions via spatially-resolved Diffusing Wave Spectroscopy (DWS)<sup>35</sup>, which determines strain associated with changes in the granular structure that occur on the order of the optical wavelength ( $10^{-6} m$ ) (see Methods). Our experimental system consists of a granular heap initially prepared (time  $t = 0$ ) just below the angle of repose, that is confined in an acrylic cell (Fig. 1) sitting on a vibration-isolating optical table (see Methods, Fig. S2). Most experiments used glass beads with ideal optical properties; however, natural sand, and a mixture of equal parts sand and kaolinite powder, were also tested (Fig. S3).

The first important result is that creep occurred for all experiments and granular materials, and it persisted over all observed timescales ( $10^0 - 10^6$  s M1-4). Initial creep velocities ( $t = 0$ ) were on the order of nm/s (cm/year) i.e., comparable to measured rates of hillslope soil creep in the field (see below) – and we confirmed that inertial numbers for undisturbed creep were all below yield ( $I < 10^{-5}$ ) (Figs. S4, S5). All experiments exhibited glass-like ‘spatially-heterogeneous dynamics’<sup>6</sup>, manifest as discrete, mesoscopic ( $\gg d$ ) zones of strain that occurred throughout the system (Fig. 1c). At early times, these deformation zones were relatively larger and more concentrated near the sandpile surface. At later times these zones became smaller and occur less frequently, with lower spatial density. Cumulative strain  $\epsilon$  resulting from this deformation diminished with depth beneath the surface because of increasing confining pressure, which restricts dilation that is often associated with grain rearrangement<sup>23,29</sup> (Fig. 4b). We also observed sensitivity to the preparation protocol, a ubiquitous phenomenon in fragile solids<sup>36</sup>. For example: the region of intense and persistent deformation seen near the pile apex (Figs. 1; 3 M1) always occurred at the location where avalanches had formed when the sand was first poured.

Information on the time-dependent dynamics of creeping motion in the pile is encoded in the correlation function  $G$  of the speckle patterns (see Methods). In the experiments reported here,  $G$  decayed monotonically with lag time  $\tau$ ; this decay was most rapid at early times  $t$  indicating fast grain motions, and slowed through time (Fig. 2). Normalizing the lag time of each correlation by the e-folding time, we find that the curves  $G(\tau/\tau_e)$  collapse onto a single exponential master curve (Fig. 2) consistent with previous observations of granular creep<sup>23</sup> and molecular dynamics simulations of glass<sup>37</sup>. The growth of the relaxation timescale  $\tau_e$  increased as a power-law function of time (Fig. 2). Such power-law ‘aging’ is a classical behavior of creeping glass and other amorphous solids<sup>7</sup>. Our interpretation is that the initially loose sandpile has many ‘soft spots’<sup>32</sup> associated with low packing density and/or frictional contacts, and that strain relaxes these soft spots, redistributing stress within the system, leading to an overall slowing down of creep with time<sup>7</sup>.

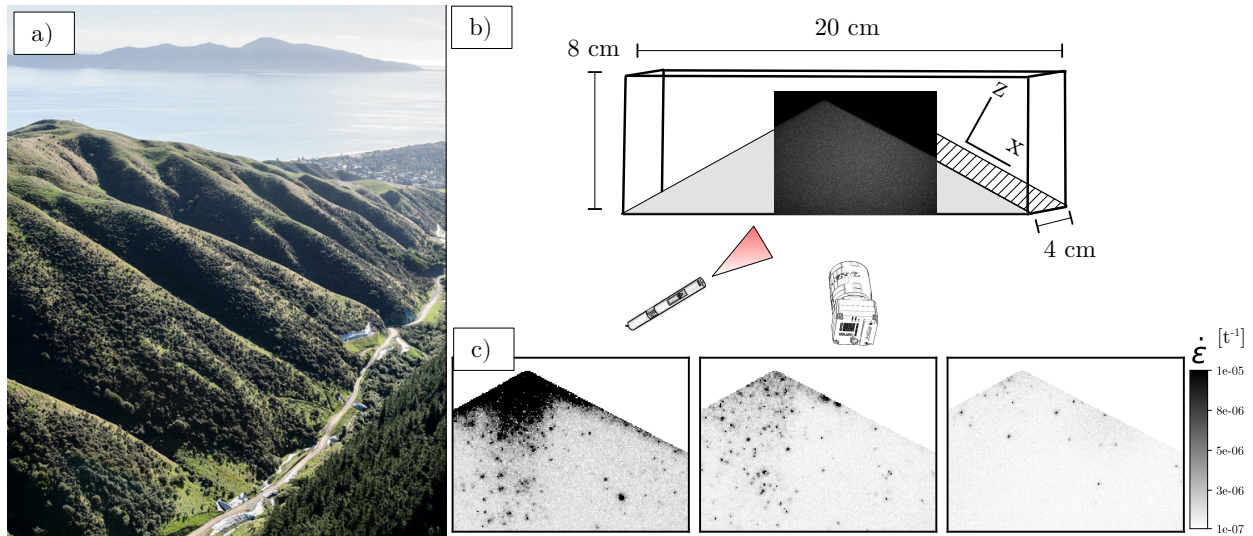


**Figure 1: Experimental setup and phenomenology.** a) Soil-mantled hillslope in the Te Puka Valley, New Zealand (PC: Waka Tokahi, NZ Transport Agency). b) Experimental DWS setup. c) Spatially-resolved maps of creep rates at three times ( $t = 1, t = 16$  and  $t = 1024$  s) since building the pile.

107

108

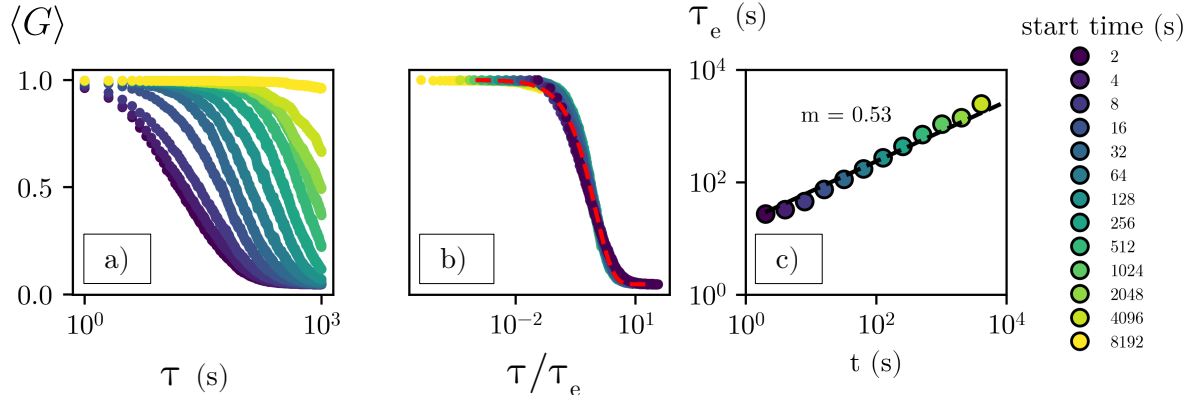


**Figure 2: Glassy relaxation in an undisturbed granular heap.** a) Spatially-averaged correlation function for 13 start times. b) Data are reasonably collapsed by  $\tau_e$ ; red dotted line indicates exponential decay. c) Growth of the relaxation timescale; slope determined from least-squares regression of  $t = t_0 \tau_e^m$ , where  $m = 0.53$ .

## 109 The role of mechanical disturbances

110 In the above description, granular creep progressively slows down. In this picture of relaxation, creep rates should  
 111 tend asymptotically toward zero with time. Not all of our experiments, however, exhibited this behavior. Humidity  
 112 fluctuations occurred for some runs, producing a complex response in terms of creep dynamics – notably at late  
 113 start times (Fig. S8). Data indicate that some reversible (elastic) strain occurred in these runs — perhaps due  
 114 to nanoscale capillary bridges or other tribological effects<sup>38,39</sup>. Similar behavior has been seen for weakly heated  
 115 granular materials<sup>35,40</sup>, suggesting that some kinds of disturbance may reverse relaxation and reactivate creep.

116 Natural hillslopes appear to creep indefinitely, and they are perpetually disturbed: bombarded by seismic waves,  
 117 thermal cycles, wetting and drying, and bioturbation<sup>8–10,16,41,42</sup>. We posit that the same relaxation processes observed  
 118 in our experiments also play out in natural soils, but that some environmental disturbances rejuvenate soil creep.  
 119 Inspired by previous work<sup>35,40</sup> we examine heating as a method for creep rejuvenation in our experiments (see  
 120 Methods). Thermal loading may be considered a proxy for shrink-swell and freeze-thaw cycles that occur in natural  
 121 soils<sup>8–10,42</sup> (see Methods). The sandpile was first allowed to relax for  $10^4$  s before applying disturbances. At the  
 122 instant heat was turned on, an increase in strain rate  $\dot{\epsilon}$  was observed as most of the pile began to creep faster (Fig. 3).  
 123 This was likely due to thermo-mechanical stresses created by volumetric expansion of the grains<sup>40</sup>, though expansion  
 124 of the apparatus walls may have also played a role. Interestingly, the spatially-averaged strain rate  $\langle \dot{\epsilon} \rangle$  (see Methods)  
 125 increased by more than ten times, reaching the same value observed at  $t = 0$ ; i.e., just after preparation of the  
 126 sandpile. Correlation functions also appeared similar to those observed at  $t = 0$  (Fig. S10). This demonstrates that a  
 127 few seconds of heating was able to reverse  $10^4$  s of aging. Once heat was switched off,  $\langle \dot{\epsilon} \rangle$  dropped immediately, then  
 128 slowly decayed toward the pre-heating value (Fig. 3a). Repeated cycles of heating and cooling produced concurrent  
 129 cycles of rejuvenation and relaxation, respectively; the overall effect was to sustain an approximately constant average  
 130 creep rate, that did not decay with time (Fig. S11). The ability of thermal cycling to sustain enhanced creep rates  
 131 has intriguing implications for natural hillslope soils.

132 Tapping of grains may induce surface flows on heaps, but also leads to compaction of the bulk<sup>43,44</sup>. Tapping may  
 133 mimic some effects of seismic shaking of hillslopes<sup>41</sup>. We allowed an initial pile to relax for  $10^4$  s, then tapped the  
 134 pile with a metronome at 1 Hz (see Methods). Taps initially excited grains throughout the pile. As time progressed,  
 135 however, a thin and fast-moving surface layer developed a sharp boundary at its base, below which the bulk grain  
 136 motions slowed dramatically and became very intermittent (Fig. 3). The development of these two regimes is similar  
 137 to the creep-flow transition observed in experiments<sup>23</sup> and simulations<sup>5</sup> of heap flows above the angle of repose (Fig.  
 138 S12). There was an overall trend of decreasing  $\langle \dot{\epsilon} \rangle$  with increasing number of taps (Fig. 3). We conclude that  
 139 vibrations fluidized surface grains but drove compaction in the bulk<sup>44</sup>, leading to more rapid relaxation (compared to  
 140 the undisturbed case) as the pile evolved toward a denser, lower-energy state (Fig. S13). We interpret the boundary  
 141 between fast and slow regions as a yield surface<sup>29</sup>. These findings may have relevance for landslide development from  
 142 earthquakes. In particular, while vibrations in our experiments excited surficial flow, the underlying bulk became  
 143 more rigid and less susceptible to future fluidization.

144

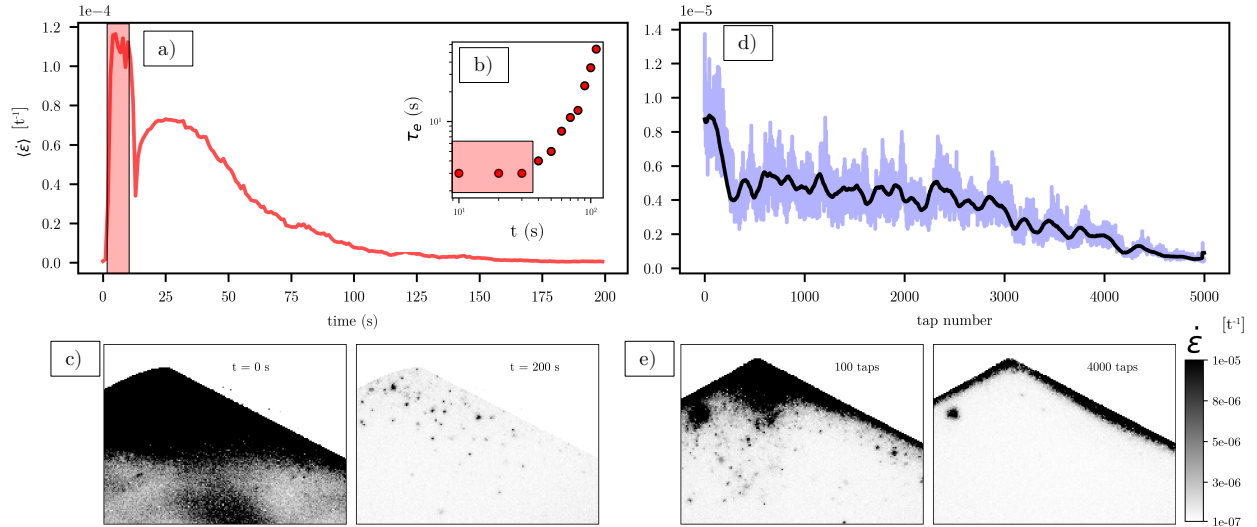


**Figure 3: Mechanical perturbations drive rejuvenation and aging.** a) Spatially-averaged strain rate including 10 s of heating applied (red rectangle) and relaxation after removal of the heat source. b) Relaxation timescale  $\tau_e$  during and following heat response (Fig. S10). c) Spatial maps of strain rate during and following heat pulse. d) Time series of spatially-averaged strain rate (blue line). Black line indicates moving-window average (100 taps). e) Spatial maps of strain rate determined over one tap cycle (tap number indicated in figure). Note that after many taps, creep is mostly confined to a thin, localized layer at surface.

## 145 Comparison with field observations

146 Field measurements of soil creep on hillslopes are quite coarse compared to our experiments. Nonetheless, profiles of  
 147 displacement, measured over decades by buried tracers in so-called ‘Young pits’ (Fig. 4a), provide a long-time average  
 148 of soil motion at discrete depths  $z$ . Horizontal velocity profiles ( $u(z)$ ) measured from a variety of environments are  
 149 typically exponential-like<sup>14,45,46</sup>, though quantitative comparisons among field sites have not been made. Here we  
 150 examine previously published field data from Young pits at four sites around the world, where creep was reportedly  
 151 driven by different forcings<sup>8–10,42</sup>. We confirm that all field data have  $I \ll 10^{-5}$ , i.e., they are in the granular creep  
 152 regime. All velocity profiles are reasonably well described by an exponential function  $u/u_0 = e^{-z/\lambda}$ , where  $u_0$  is the  
 153 surface velocity and  $\lambda$  is a decay length determined from data fitting (Figs. 4c, S6). The latter two parameters must  
 154 be related to site-specific soil characteristics and environmental disturbance regimes, but exploring this is beyond the  
 155 scope of this paper. For these hillslopes  $u_0 \sim 10^{-9}$  m/s (Figs. 4c, S6), comparable to our measured experimental  
 156 creep rates for the initially loose and heated grains.

157 We compare our undisturbed creep experiments to field data, by first generating depth ( $z$ ) profiles of downslope  
 158 ( $x$ )-averaged cumulative strain through time from the surface to 1-cm below (Fig. 4b). Our experiments permit  
 159 determination of strain rate rather than velocity (see Supplementary Materials Section S5); however, the normalized  
 160 strain rate profile  $\dot{\epsilon}/\dot{\epsilon}_0 = e^{-z/\lambda}$  is essentially equivalent to a normalized velocity profile. We see that our experimental  
 161 data fall on top of the field profiles (see Fig. S3 for experiments with other materials). It is important to note, however,  
 162 that while exponential profiles have been reported for granular creep in many experiments<sup>23,25,26</sup>, an exponential  
 163 profile is not diagnostic of creep. Inertial flows may also exhibit exponential velocity profiles<sup>22,28</sup>. Also, creep in  
 164 highly heterogeneous soils, or soils with macro-scale disturbances such as tree throw<sup>47</sup>, can exhibit erratic velocity  
 165 profiles that are not well fit by an exponential.

166

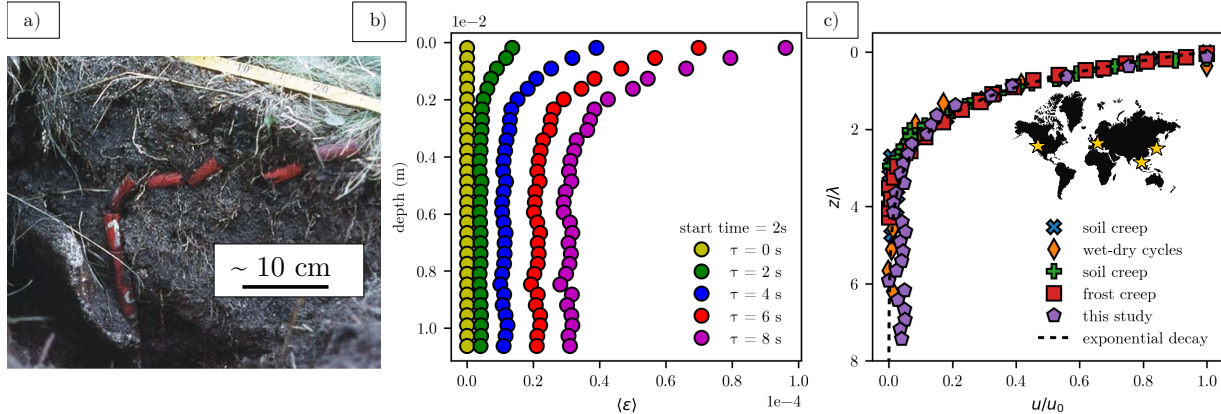


**Figure 4: Depth-averaged strain profiles from the lab and field.** a) Excavated Young Pit indicating the displacement of tracer pegs over a 17-year interval (PC Alfred Jahn). b) Depth and horizontally-averaged cumulative strain profiles at three lag times, measured in an undisturbed creep experiment. Profiles start at 2048 s after deposition. c) Compilation of soil deformation data from four studies and field environments - originally compiled by Roering<sup>46</sup>. Freeze-thaw cycles near Strasbourg, France<sup>8</sup>, wet-dry cycles in Kuala Lumpur, Malaysia<sup>42</sup>, freeze-thaw cycles in the Japanese Alps<sup>9</sup>, wet-dry cycle in Stanford, California<sup>10</sup>. Data are fit by an exponential decay, the parameters of which are then used to reasonably collapse the data (Fig. S6)

## Discussion and outlook

167

168 By probing a seemingly static sandpile with speckle imaging, our experiments have revealed a seething and ceaseless  
 169 creeping motion — even in the near absence of mechanical disturbances. These motions are strikingly similar to  
 170 recent observations of creep in a heap of Brownian (micron-scale) particles<sup>48</sup>, even though our sand grains are non-  
 171 Brownian. Further, we have shown how granular creep rates can be tuned by imposing external disturbances that  
 172 are geophysically relevant. Our experiments reveal deep similarities in how grains and glasses creep, and provide  
 173 compelling evidence that mechanical disturbances in granular systems play a role akin to thermal fluctuations in  
 174 glasses<sup>7,27,34</sup>.

175 Intriguingly, even though the mechanics of grain motion are fundamentally different from Culling’s model, our  
 176 final result provides a kind of confirmation of his physical intuition<sup>3</sup>. In particular: heterogeneity in granular structure  
 177 leads to seemingly random grain motions that decrease with depth; and mechanical disturbances can introduce new  
 178 stresses and/or porosity that facilitate motion. Creep motions are consistent with granular self diffusion<sup>49</sup>; however,  
 179 this does not imply that there is any Culling-like diffusion relation between flux and slope. Moreover, Culling and  
 180 subsequent hillslope researchers did not anticipate persistent creep even in the (near) absence of disturbance. How  
 181 do we understand the similarity in creep rates and profiles between our undisturbed and initially loose sandpile,  
 182 and natural (disturbed) hillslope soils? Our new view separates creep into a generic relaxation process whose rate  
 183 depends on granular friction/cohesion and structure, and diverse rejuvenation processes associated with environmental  
 184 disturbances. We speculate that the primary role of biophysical disturbance in natural hillslopes is to maintain soil in  
 185 a loose and fragile state, where relaxation rates are high. Other types of disturbance, however, can have the opposite  
 186 effect; shaking can lead to compaction and enhanced aging, depressing bulk creep rates even as surface motions are  
 187 enhanced.

188 Although soil is sensitive to disturbances, geologic history, and boundary effects<sup>5,27</sup>, qualitative creep dynamics  
 189 are robust across materials and environments. Future granular simulations could be used to reveal how disturbances  
 190 influence the contact forces and/or structure that ultimately drive creep. Experiments could examine the consequences  
 191 of cohesion/adhesion, surface charge, moisture, bioturbation and other effects on creep dynamics. Resolving these  
 192 factors will allow derivation of a coarse-grained creep rheology model, whose kinematics and scales are determined by  
 193 physically-meaningful parameters. Our results indicate that elastoplastic models developed to describe the rheology  
 194 of amorphous solids<sup>7</sup> — that can explicitly incorporate mesoscopic scales of grain rearrangements, and rejuvenation  
 195 by mechanical noise — may be good candidates. An improved model of soil creep is not only useful for predicting  
 196 hillslope sediment transport; it will also help us to better understand how creeping soil accelerates to the yield point,  
 197 which leads to catastrophic landslides<sup>5</sup>.

## References

- 198 1. Davis, W. M. The convex profile of bad-land divides. *Science* **6**, 245–245 (1892).
- 199 2. Gilbert, G. K. The Convexity of Hilltops. *The Journal of Geology* **17**, 344–350 (1909).
- 200 3. Culling, W. E. H. Soil Creep and the Development of Hillside Slopes. *The Journal of Geology* **71**,  
201 127–161 (1963).
- 202 4. Roering, J. J., Perron, J. T. & Kirchner, J. W. Functional relationships between denudation and hillslope  
203 form and relief. *Earth and Planetary Science Letters* **264**, 245–258 (2007).
- 204 5. Ferdowsi, B., Ortiz, C. P. & Jerolmack, D. J. Glassy dynamics of landscape evolution. *Proceedings of  
205 the National Academy of Sciences* **115**, 4827–4832 (2018).
- 206 6. Falk, M. L. & Langer, J. S. Dynamics of viscoplastic deformation in amorphous solids. *Physical Review  
207 E - Statistical Physics, Plasmas, Fluids, and Related Interdisciplinary Topics* **57**, 7192–7205 (1998).
- 208 7. Nicolas, A., Ferrero, E. E., Martens, K. & Barrat, J.-L. Deformation and flow of amorphous solids:  
209 Insights from elastoplastic models. *Reviews of Modern Physics* **90**, 45006 (2018).
- 210 8. Auzet, A. V. & Ambroise, B. Soil creep dynamics, soil moisture and temperature conditions on a  
211 forested slope in the granitic vosges mountains, France. *Earth Surface Processes and Landforms* **21**,  
212 531–542 (1996).
- 213 9. Matsuoka, N. The relationship between frost heave and downslope soil movement: field measurements  
214 in the Japanese Alps. *Permafrost and Periglacial Processes* **9**, 121–133 (1998).
- 215 10. Fleming, R. W. & Johnson, A. M. Rates of seasonal creep of silty clay soil. *Quarterly Journal of  
216 Engineering Geology and Hydrogeology* **8**, 1–29 (1975).
- 217 11. Whipple, K. X., Kirby, E. & Brocklehurst, S. H. Geomorphic limits to climate-induced increases in  
218 topographic relief. *Nature* **401**, 39–43 (1999).
- 219 12. Dietrich, W. E. & Perron, J. T. The search for a topographic signature of life. *Nature* **439**, 411–418  
220 (2006).
- 221 13. Perron, J. T., Kirchner, J. W. & Dietrich, W. E. Formation of evenly spaced ridges and valleys. *Nature*  
222 **460**, 502–505 (2009).
- 223 14. Young, A. Soil movement by denudational processes on slopes. *Nature* **188**, 120–122 (1960).
- 224 15. Kirkby, M. J. Hillslope process-response models based on the continuity equation. *Inst. Br. Geogr. Spec.  
225 Publ* **3**, 5–30 (1971).
- 226 16. Gabet, E. J. Gopher bioturbation: Field evidence for non-linear hillslope diffusion. *Earth Surface Pro-  
227 cesses and Landforms* **25**, 1419–1428 (2000).
- 228 17. Dietrich, W. E. *et al.* Geomorphic transport laws for predicting landscape form and dynamics. *Geo-  
229 physical Monograph Series* **135**, 103–132 (2003).
- 230 18. Roering, J. J., Kirchner, J. W., Sklar, L. S. & Dietrich, W. E. Hillslope evolution by nonlinear creep  
231 and landsliding: An experimental study. *Geology* **29**, 143–146 (2001).
- 232 19. Furbish, D. J., Schmeeckle, M. W. & Roering, J. J. Thermal and force-chain effects in an experimental,  
233 sloping granular shear flow. *Earth Surface Processes and Landforms* **33**, 2108–2117 (2008).
- 234 20. Gray, H. J., Keen-Zebert, A., Furbish, D. J., Tucker, G. E. & Mahan, S. A. Depth-dependent soil mixing  
235 persists across climate zones. *Proceedings of the National Academy of Sciences*, 201914140 (2020).
- 236 21. Roering, J. J., Kirchner, J. W. & Dietrich, W. E. Hillslope evolution by nonlinear, slope-dependent  
237 transport: Steady state morphology and equilibrium adjustment timescales. *Journal of Geophysical  
238 Research: Solid Earth* **106**, 16499–16513 (2001).
- 239 22. Jop, P., Forterre, Y. & Pouliquen, O. A constitutive law for dense granular flows. *Nature* **441**, 727–730  
240 (2006).
- 241 23. Katsuragi, H., Abate, A. R. & Durian, D. J. Jamming and growth of dynamical heterogeneities versus  
242 depth for granular heap flow. *Soft Matter* **6**, 3023–3029 (2010).
- 243

- 244 24. Ferdowsi, B., Ortiz, C. P., Houssais, M. & Jerolmack, D. J. River-bed armouring as a granular segregation phenomenon. *Nature Communications* **8** (2017).  
245
- 246 25. Komatsu, T. S., Inagaki, S., Nakagawa, N. & Nasuno, S. Creep Motion in a Granular Pile Exhibiting  
247 Steady Surface Flow. *Physical Review Letters* **86**, 1757–1760 (2001).
- 248 26. Houssais, M., Ortiz, C. P., Durian, D. J. & Jerolmack, D. J. Rheology of sediment transported by a  
249 laminar flow. *Physical Review E* **94**, 1–10 (2016).
- 250 27. Jerolmack, D. J. & Daniels, K. E. Viewing Earth’s surface as a soft-matter landscape. *Nature Reviews*  
251 *Physics* **1**, 716–730 (2019).
- 252 28. Kamrin, K. & Koval, G. Nonlocal constitutive relation for steady granular flow. *Physical Review Letters*  
253 **108** (2012).
- 254 29. Amon, A., Bertoni, R. & Crassous, J. Experimental investigation of plastic deformations before a  
255 granular avalanche. *Physical Review E - Statistical, Nonlinear, and Soft Matter Physics* **87**, 1–12 (2013).
- 256 30. Allen, B. & Kudrolli, A. Granular bed consolidation, creep, and armoring under subcritical fluid flow.  
257 *Physical Review Fluids* **7**, 1–21 (2018).
- 258 31. BenDror, E. & Goren, L. Controls Over Sediment Flux Along Soil-Mantled Hillslopes: Insights From  
259 Granular Dynamics Simulations. *Journal of Geophysical Research: Earth Surface* **123**, 924–944 (2018).
- 260 32. Liu, A. J. & Nagel, S. R. The Jamming Transition and the Marginally Jammed Solid. *Annual Review*  
261 *of Condensed Matter Physics* **1**, 347–369 (2010).
- 262 33. Scalliet, C. & Berthier, L. Rejuvenation and Memory Effects in a Structural Glass. *Physical Review*  
263 *Letters* **122**, 255502 (2019).
- 264 34. Agoritsas, E., García-García, R., Lecomte, V., Truskinovsky, L. & Vandembroucq, D. *Driven Interfaces:*  
265 *From Flow to Creep Through Model Reduction* **6**, 1394–1428 (Springer US, 2016).
- 266 35. Amon, A., Mikhailovskaya, A. & Crassous, J. Spatially resolved measurements of micro-deformations  
267 in granular materials using diffusing wave spectroscopy. *Review of Scientific Instruments* **88** (2017).
- 268 36. Vanel, L., Howell, D., Clark, D., Behringer, R. P. & Clément, E. Memories in sand: Experimental tests  
269 of construction history on stress distributions under sandpiles. *Physical Review E - Statistical Physics,*  
270 *Plasmas, Fluids, and Related Interdisciplinary Topics* **60**, 5040–5043 (1999).
- 271 37. Berthier, L. & Barrat, J. L. Shearing a Glassy Material: Numerical Tests of Nonequilibrium Mode-  
272 Coupling Approaches and Experimental Proposals. *Physical Review Letters* **89**, 1–4 (2002).
- 273 38. Royer, J. R. *et al.* High-speed tracking of rupture and clustering in freely falling granular streams.  
274 *Nature* **459**, 1110–1113 (2009).
- 275 39. Zaitsev, V. Y., Gusev, V. E., Tournat, V. & Richard, P. Slow relaxation and aging phenomena at the  
276 nanoscale in granular materials. *Physical Review Letters* **112**, 1–5 (2014).
- 277 40. Djaoui, L. & Crassous, J. Probing creep motion in granular materials with light scattering. *Granular*  
278 *Matter* **7**, 185–190 (2005).
- 279 41. Bontemps, N., Lacroix, P., Larose, E., Jara, J. & Taïpe, E. Rain and small earthquakes maintain a  
280 slow-moving landslide in a persistent critical state. *Nature Communications* **11**, 1–10 (2020).
- 281 42. Eyles, R. J. & Ho, R. Soil creep on a humid tropical slope. *Journal of Tropical Geography* **31**, 40–42  
282 (1970).
- 283 43. Richard, P., Nicodemi, M., Delannay, R., Ribi ere, P. & Bideau, D. Slow relaxation and compaction of  
284 granular systems. *Nature Materials* **4**, 121–128 (2005).
- 285 44. Iikawa, N., Bandi, M. M. & Katsuragi, H. Force-chain evolution in a two-dimensional granular packing  
286 compacted by vertical tappings. *Physical Review E* **97**, 1–10 (2018).
- 287 45. Kirkby, A. M. J. Measurement and Theory of Soil Creep. *The Journal of Geology* **75**, 359–378 (1967).
- 288 46. Roering, J. J. Soil creep and convex-upward velocity profiles: Theoretical and experimental investigation  
289 of disturbance-driven sediment transport on hillslopes. *Earth Surface Processes and Landforms* **29**,  
290 1597–1612 (2004).



- 291 47. Gabet, E. J., Reichman, O. & Seabloom, E. W. The Effects of Bioturbation on Soil Processes and  
 292 Sediment Transport. *Annual Review of Earth and Planetary Sciences* **31**, 249–273 (2003).
- 293 48. Bérut, A., Pouliquen, O. & Forterre, Y. Brownian Granular Flows Down Heaps. *Physical Review Letters*  
 294 **123**, 1–5 (2019).
- 295 49. Fan, Y., Umbanhowar, P. B., Ottino, J. M. & Lueptow, R. M. Shear-Rate-Independent Diffusion in  
 296 Granular Flows. *Physical Review Letters* **115**, 1–5 (2015).

## 297 **Methods and protocols**

### 298 **Measuring grain motion**

299 The principle of DWS is that highly coherent light illuminates our granular heap, where photons scatter and interfere,  
 300 which produces a random ‘speckle pattern’ that is collected with a CCD camera (Fig. 1, Supplementary Material  
 301 S3). As grains slowly creep past one another, they change the photon trajectories and render new speckle patterns.  
 302 We achieve spatially-resolved measurements by partitioning images into a grid with cells (metapixels) of size  $l^*$ , the  
 303 mean free path of photons within the material. This quantity is around  $l^* \approx 3d$  for the granular materials used (see  
 304 Methods). Fluctuations in the speckle pattern between a start time  $t$  and a lag time  $\tau$  within each metapixel are  
 305 quantified via the normalized correlation function,  $G(t, \tau)$  (Fig. 2)<sup>35</sup>. Global dynamics across the whole sandpile  
 306 are measured by averaging  $G$  for each metapixel, signified as  $\langle G \rangle$ . This allows determination of the first important  
 307 quantity for assessing glassy dynamics: the relaxation time  $\tau_e$ , determined as the time at which  $\langle G \rangle = 1/e$  (Fig.  
 308 2). For most experiments we used monodisperse glass beads (Cerroglass), of diameter  $d_s = 100\mu\text{m}$  and density  $\rho =$   
 309  $2.6\text{ g/cc}$ , to build the sandpile. This material was chosen because its scattering properties are well understood and  
 310 it is standard in DWS experiments. From the correlation function  $G$ , we can apply optical theory<sup>35</sup> to determine  
 311 the second important quantity for examining glassy dynamics:  $\epsilon$ , the strain that occurs within a volume set by  $l^*$   
 312 (see Supplemental Materials Section S3). Whereas DWS can still be used to examine relative grain motions for the  
 313 sand and clay mixtures we used, use of more complex materials precludes us from calculating  $l^*$  and hence from  
 314 determining absolute strain  $\epsilon$  (Supplementary Material S5).

### 315 **Experimental procedures**

316 Our experimental system is not meant to be a scaled model of a hillslope, either in a geometric or dynamic sense.  
 317 Rather, it is designed to optimize the direct observation of grain motions, in order to understand the granular physics  
 318 of creep that are relevant for soil motion at the pedon scale in nature. Reported experiments were conducted in  
 319 relatively constant ambient temperature ( $21\text{C} \pm 0.2$ ) and relative humidity ( $23.8\% \pm 0.3$ ) conditions (Fig. S7).  
 320 The heap was prepared by allowing a fixed volume/flow rate of granular material (well within the continuous-flow  
 321 regime<sup>22</sup>) to flow out of a funnel, at a fixed height 8 cm above the center of the cell bottom. Results are reported  
 322 for glass beads, unless otherwise stated. Our ‘undisturbed’ experiments consisted of allowing the initial pile to relax  
 323 under gravity, with no imposed external disturbances. We note, however, that small-scale ambient fluctuations in  
 324 temperature and relative humidity did occur (Fig. S7). We conducted a ‘short’ duration experiment at a frame rate  
 325 of  $f = 1\text{Hz}$  for  $10^4$  seconds (2.8 hours) immediately following preparation, and a ‘long’ duration experiment with  
 326  $f = 0.2\text{Hz}$  for  $10^6$  seconds (11 days). Image collection began at the start of emptying the funnel, while analysis  
 327 of creep dynamics reported here started as the last grain entered the system and avalanching ceased ( $t = 0$ ) —  
 328 making the initial condition a sandpile prepared just below the angle of repose (Fig. 1). We computed both the  
 329 instantaneous strain rate determined from successive image pairs through time,  $\dot{\epsilon}(\tau = 1\text{s}) = \epsilon(t)f$  (e.g., Fig. 1),  
 330 and the temporal evolution of the relaxation timescale  $\tau_e$  sampled from different start times  $t$ , for each metapixel  
 331 in an image. From these we generated ensemble-average values for each image,  $\langle \dot{\epsilon} \rangle$  and  $\langle \tau_e \rangle$ , that characterized the  
 332 spatially-averaged dynamics of the sandpile through time (Figs. 1, 2, 3). From instantaneous strain values we also  
 333 computed surface-normal ( $z$ ) profiles of downslope ( $x$ )-averaged strain (Figs. S4, S5); this allowed us to generate  
 334 depth profiles of cumulative strain through time, for comparison to field data (Fig. 4).

## 335 Disturbance protocols

336 For experiments with disturbance, a pile prepared following the protocol above was allowed to relax for  $10^4$  s before  
337 disturbances began. Heating of glass beads produces a small but measurable volume expansion<sup>40</sup> (coefficient of  
338 thermal expansion  $\sim 10^{-6} K^{-1}$ ) that is reversed as grains cool. At  $t = 0$  heat was applied to the side of the cell for  
339 10 s by a heat gun, producing a measured sidewall temperature of 50C (Fig. S9). After 10 s the heating element  
340 was removed, while the creep response was documented for another 200 s (Fig. 3). For tapping experiments, discrete  
341 taps were delivered to the pile using a metronome (double pendulum) that rests on a platform attached to the cell  
342 (Fig. S9). At  $t = 0$  we initiated a series of 5000 taps delivered at a rate of 1 Hz, and recorded images at the same  
343 rate — but phase-lagged from the taps — for the 5000-s duration (Figs. 3, S9).

344 **Acknowledgements:** We thank L. Galloway, A. Gunn and D.J. Durian for helpful discussions, and ARO W911NF-  
345 20-1-0113 for financial support.

346 **Author contributions:** N.S.D performed the experiments and analysis; D.J.J. supervised the research; all authors  
347 contributed to interpretation and writing.

348 **Competing interest statement:** The authors declare no competing interests.

349 **Additional information:** Extended data figures and methods are included in Supplementary Materials.

350 **Data availability statement:** Data will be deposited in the publicly shared repository figshare, and all code used  
351 to analyze these data will be publicly available on github.